

## Fourier relationship between the angle and angular momentum of entangled photons

A. K. Jha,<sup>1</sup> B. Jack,<sup>2</sup> E. Yao,<sup>2</sup> J. Leach,<sup>2</sup> R. W. Boyd,<sup>1</sup> G. S. Buller,<sup>3</sup> S. M. Barnett,<sup>4</sup> S. Franke-Arnold,<sup>2</sup> and M. J. Padgett<sup>2,\*</sup>

<sup>1</sup>*Institute of Optics, University of Rochester, Rochester, New York 14627, USA*

<sup>2</sup>*Department of Physics and Astronomy, SUPA, University of Glasgow, Glasgow, United Kingdom*

<sup>3</sup>*School of Engineering and Physical Sciences, SUPA, Heriot-Watt University, Riccarton, Edinburgh, United Kingdom*

<sup>4</sup>*Department of Physics, SUPA, University of Strathclyde, Glasgow, United Kingdom*

(Received 28 April 2008; published 8 October 2008)

We study the Fourier relationship between angle and orbital angular momentum of entangled photons. Spatial light modulators allow us to define and control the spatial mode measurement state. We observe strong quantum correlations, establishing that angular position and momentum distributions between the photons are related as conjugate Fourier pairs.

DOI: 10.1103/PhysRevA.78.043810

PACS number(s): 42.50.Dv, 03.67.Bg

### I. INTRODUCTION

Experiments with correlated photon pairs have played an essential role in demonstrating the nonlocal nature of quantum mechanics, confirming the existence of entanglement in nature [1,2]. Today entanglement is very much a resource to be exploited, with practical applications in NMR [3] and exciting possibilities in quantum information processing [4].

The first entanglement experiments were based on the correlations in the polarizations of photon pairs produced from a cascade transition [1,2]. More recent experiments have exploited photon pairs generated in parametric down conversion where phase matching induces wave-vector-position entanglement [5,6]. These momentum-position relationships extend entanglement phenomena beyond polarization to include continuous variables. For example, placing a diffraction slit in one arm produces “ghost diffraction” where the slit diffraction pattern is observed in neither of the beams independently, but only in their coincidence count [7]. It is a feature of entangled systems that they exhibit correlations not just for one property, but also in a conjugate variable. A recent demonstration of the entanglement between down-converted photon pairs is the measurement of both the position and momentum correlations, thus realizing the original Einstein-Podolsky-Rosen (EPR) *Gedankenexperiment* [8].

Apart from polarization, i.e., spin angular momentum, light also possesses an orbital angular momentum (OAM),  $\ell\hbar$  per photon arising from a helical phase structure,  $\exp(i\ell\phi)$ , of the beam [9,10]. This angular momentum is independent of the polarization of the beam. In 2001, correlations were observed in the measured OAM states of down-converted photon pairs [11], confirming that the OAM of light is a property of single photons [12]. More recent experiments have shown that these correlations persist for non-integer OAM states [13].

We explore the relationship between OAM and its conjugate variable, angular position [14]. Given a Fourier relationship between OAM and angular position [15,16], we can write the amplitudes of the OAM states,  $A_\ell$ , and the azimuthal dependence of the corresponding complex beam am-

plitude,  $\Psi(\phi)$ , as generation functions of each other,

$$A_\ell = \frac{1}{\sqrt{2\pi}} \int_{-\pi}^{\pi} \Psi(\phi) \exp(-i\ell\phi) d\phi, \quad (1)$$

$$\Psi(\phi) = \frac{1}{\sqrt{2\pi}} \sum_{\ell=-\infty}^{\infty} A_\ell \exp(i\ell\phi). \quad (2)$$

In this article, we establish that this relationship applies not just to a single classical light beam but also to correlations between down-converted photon pairs, i.e., that setting the angular mode of one photon dictates the OAM distribution of the other. This effect may be termed “angular ghost diffraction.”

While both linear position and momentum are continuous and unbounded variables, angle is  $2\pi$  periodic. This leads to a natural quantization of angular momentum, and because of the bounded nature of the angular variable, care is required in calculating the angular uncertainty. Nevertheless, it has been possible to derive a rigorous uncertainty relation directly from the Fourier relationship between angular momentum and angular position [15–18].

### II. MEASURING SINGLE-PHOTON OAM

Single-photon detectors can be used with polarizing beam splitters and wave plates to discriminate between any two orthogonal polarization states. The efficient measurement of OAM is not so straightforward. Spin, orbital, and total angular momentum can be measured interferometrically [19], but to cover many states is technically complicated. More conveniently OAM states can be measured using a “forked diffraction grating” (i.e., hologram) [20] to selectively couple a specific OAM state into a single-mode fiber [11]. Only a single OAM state can be measured at any one time, but the technique is sufficient for experiments that do not require a high quantum yield. Rather than using interchangeable holograms, one can use spatial light modulators (SLMs) to implement the various holograms, thereby easing the alignment and automation of such experiments [21,22].

\*m.padgett@physics.gla.ac.uk

**III. THEORY**

Each of the down-converted beams is spatially incoherent [23] and, in terms of its OAM, has a distribution of states symmetric about  $\ell=0$  [24]. The width of this distribution is set by the size of the pump beam with respect to the size of the OAM states, which scales with  $\sqrt{\ell}$  [25]. It follows that the count rate from a single detector as a function of  $\ell$  is a similarly broad function [26]. The coincidence count rate  $C$  is proportional to the overlap between the transverse mode amplitudes of the two down-converted beams  $A$  and  $B$  with that of the pump ( $P$ ) [27],

$$C \propto \frac{|\int \Psi_A \Psi_B \Psi_P^* dA|^2}{\sqrt{\int |\Psi_A \Psi_P^*|^2 dA} \sqrt{\int |\Psi_B \Psi_P^*|^2 dA}}. \quad (3)$$

For a planar-waved pump beam,  $\ell_P=0$ , with a diameter larger than the back-projected down-converted beams, the coincidence count reduces to the simpler form

$$C \propto \left| \int \Psi_A \Psi_B dA \right|^2. \quad (4)$$

For OAM states of the two down-converted beams that are within a few degrees of being collinear [28] this becomes

$$C \propto \left| \int \Psi_A(r) \exp(i\ell_A \phi) \Psi_B(r) \exp(i\ell_B \phi) r dr d\phi \right|^2, \quad (5)$$

which, due to the orthogonality of OAM states, is nonzero only when  $\ell_A + \ell_B = 0$ .

If a Fourier relationship between angle and OAM is valid for photon pairs, then an aperture with a transmission that is solely a function of its azimuthal angle inserted into optical arm  $B$  should create a nonzero coincidence rate with respect to a range of  $\ell_A$  as measured in arm  $A$ . Such an aperture can be expressed as the sum of its angular harmonics with Fourier coefficients  $B_n$  [15],

$$M(\phi) = \sum_{n=-\infty}^{\infty} B_n \exp(in\phi). \quad (6)$$

Combining multiple apertures to give an  $m$ -fold rotationally symmetric pattern means that  $B_n$  is nonzero only if  $n$  is an integer multiple of  $m$ . For hard-edged apertures, with an open segment width  $\Theta$ ,  $M(\phi)=1$  for  $-\Theta/2 < \phi + 2\pi N/m \leq \Theta/2$  and  $M(\phi)=0$  otherwise. These nonzero  $B_n$  components are

$$B_{n=Nm} = \frac{m\Theta}{2\pi} \text{sinc}\left(\frac{n\Theta}{2}\right). \quad (7)$$

The action of this mask on an OAM eigenstate produces a distribution of OAM values with amplitudes for the induced change in  $\ell$  given by the  $B_n$ . As the individual light beams are spatially incoherent, this distribution is not recorded in the single channel counts. OAM conservation requires that if we pass one of the down-converted beams through the mask and then measure the OAM for both, we should always find that the sum of the recorded OAM values is an integer multiple of  $m$ . More specifically, the coincidence count will take the form

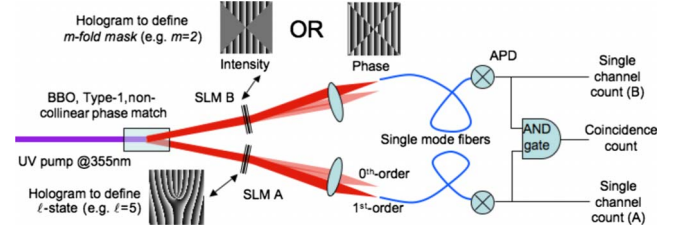


FIG. 1. (Color online) Experimental apparatus. A frequency tripled Nd:yttrium-aluminum-garnet (Nd:YAG) laser at 355 nm is incident on a beta barium borate (BBO) crystal producing photon pairs at 710 nm. Signal and idler photons are coupled using single mode fiber to avalanche photodiodes. Both the single channel and coincidence count rates are recorded as functions of the hologram design displayed on the spatial light modulator(s).

$$C_{\ell_A=Nm} \propto \left| \frac{m\Theta}{2\pi} \text{sinc}\left(\frac{\ell_A \Theta}{2}\right) \right|^2. \quad (8)$$

For the special case of equally sized open and closed segments ( $\Theta = \pi/m$ ) we have

$$C_{\ell_A=Nm} \propto \left| \frac{1}{2} \text{sinc}\left(\frac{\ell_A \pi}{2m}\right) \right|^2. \quad (9)$$

In nonlocal experiments of this type, the coincidence count rate can be predicted by “back projection” [29] or “retro-diction” [30] techniques. One of the detectors is considered to be a source of photons which propagate back through the optical components of one optical arm to be phase-conjugately reflected by the nonlinear crystal, and transmitted along the other optical arm to the second detector. The probability of detection at this second detector is proportional to the predicted coincidence count rate of the true quantum experiment. However, this retrodiction is purely a predictor of outcome, not a mechanism, and within this back projection approach the detector events are not coincident.

**IV. EXPERIMENTAL APPARATUS**

Figure 1 shows a schematic diagram of the experimental apparatus. The down-conversion source is a frequency-tripled, mode-locked, Nd:YAG laser (Excyte) with a pulse repetition frequency of 100 MHz and an average power of 150 mW at  $\approx 355$  nm. The 2 mm diameter collimated pump beam is normally incident on a 3 mm long crystal of BBO, cut for frequency degenerate type-1 noncollinear phase matching with a semicone angle for the down-converted beams of  $4^\circ$ . The single photon detection is by avalanche photodiodes (Perkin Elmer) with quantum efficiencies of about 60%, both connected to single mode fibers. The input facets of the fibers are imaged, with a magnification of approximately 20:1, using high quality 60 mm focal length lenses to overlap with each other and the pump beam at the output facet of the crystal. The transistor-transistor logic outputs of the two detectors are each counted independently and their coincidence counts are recorded (National Instruments PCI-6602). In both of the down-converted arms, electrically addressed, phase-only SLMs (Hamamatsu) are incorporated,

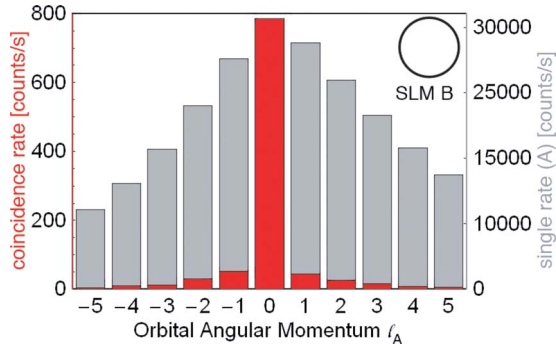


FIG. 2. (Color online) Coincidence counts (red; dark gray in printed version) and single channel counts (gray) in channel (A) as functions of  $\ell_A$  for the case that no aperture is implemented on SLM B. Note that the distribution of detected  $\ell$  states for the single channel (A) is broad, but the coincidence count rate is only substantial for  $\ell_A=0$ . The single channel count rate in channel (B) is independent of  $\ell_A=0$  (not shown).

on which various holograms can be displayed, thereby setting the measurement state of the detected photons. Both the single channels and coincidence counts are recorded as a function of the hologram designs.

The hologram designs in this work use a modulation of the phase depth so that the phase-only SLM can impart both phase and intensity modulation to the diffracted light [31,32]. The hologram design for measuring the OAM state is the standard  $\ell$ -forked diffraction grating. The angular mask is obtained as the product of an  $\ell=0$  hologram with the  $m$ -fold rotationally symmetric mask, which can be either an intensity or phase mask (see Fig. 1).

## V. EXPERIMENTAL RESULTS

Figure 2 shows the measured single channel and coincidence counts for the case that no angular mask was present in the optical path B. The single channel (A) counts reflect the efficiency of the down-conversion process to generate different OAM modes which decreases with increasing  $|\ell|$ . The single count rate in channel (B) of course is not affected by the SLM in channel (A) and remains constant. The count rate on the two single channels was of order  $25\,000\text{ s}^{-1}$ . For  $\ell_A=0$  the coincidence count rate was approximately  $750\text{ s}^{-1}$ , implying an overall quantum detection efficiency of 3% and a photon pair rate of about  $10^6\text{ s}^{-1}$ , meaning that the contribution to the coincidence count from multiple photon pairs can be ignored. The gate time of the detection electronics and coincidence counting was 25 ns, which for the observed single channel count rates gives an accidental, i.e., nonquantum coincidence rate of  $3\text{ s}^{-1}$ . The hologram in optical path A could then be updated and the various count rates recorded as a function of different  $\ell$  states.

The SLM B was then modified to incorporate an annular,  $m$ -twofold rotationally symmetric intensity mask, and a similar scan of the  $\ell$  state was completed. Figure 3 shows our results for single channel (A) and coincidence channel counts as functions of  $\ell_A$ . Of particular significance is that whereas the single channel count has a broad spectrum, the

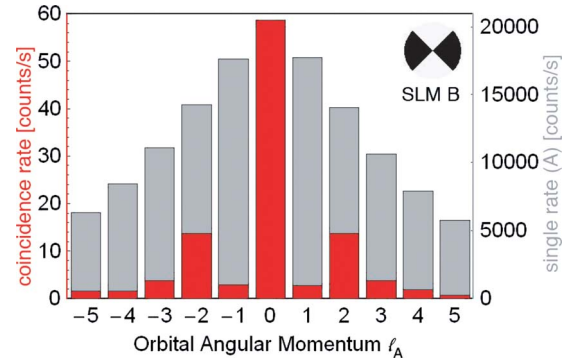


FIG. 3. (Color online) Coincidence counts (red; dark gray in printed version) and single channel counts (gray) in channel (A) as functions of  $\ell_A$  for the case that a twofold rotationally symmetric intensity aperture ( $m=2$ ) is implemented on SLM B. Note that the distribution of detected  $\ell$  states for the single channel is broad, but the coincidence count shows distinct sidebands for  $\ell_A = \pm 2$ .

coincidence count shows noticeable sidebands at  $\ell_A = \pm 2$ . Note that the sinc envelope suppresses any coincidence counts at  $\ell_A = \pm 4$ , as expected from Eq. (9). Further sidebands in the coincidence counts would be expected at  $\ell_A = \pm 6$ , but were barely observable above the background noise.

The intensity aperture implemented on SLM B can be replaced with a phase aperture where alternate sectors induce a phase delay of  $\pi$ . The equal mark-space ratio of the  $\pi$ -phased aperture means that  $B_{n=0}=0$  and hence that the coincidence count for  $\ell_A=0$  is suppressed. Figure 4 shows the coincidence and single channel (A) counts for an  $m=2$  phase mask on SLM B and OAM state measurement on SLM A, as a function of  $\ell_A$ . We see clearly a high coincidence count rate for  $\ell_A = \pm 2$ , whereas the single channel (A) count shows no such peaks.

## VI. CONCLUSIONS

We have established that the Fourier relationship between angular position and OAM holds for entangled photon pairs produced by a down-conversion source. Confirming this

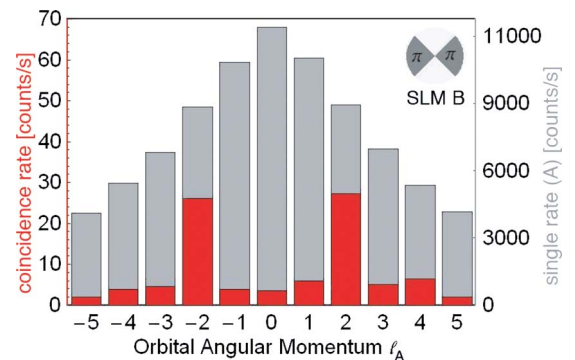


FIG. 4. (Color online) As in Fig. 3, but for a twofold rotationally symmetric phase aperture implemented on SLM B. The coincidence count shows distinct sidebands for  $\ell_A = \pm 2$  and a suppression of the count rate at  $\ell_A=0$ .

Fourier relationship between pairs of separated photons has implications for the validity of an angular form of the Heisenberg uncertainty relationship [18], which is itself a direct consequence of the Fourier relationship. A demonstration of angular entanglement supports the quantum nature of the azimuthal coordinate itself [14]. Although the separation of our detectors was too small with respect to our gate times for our results to constitute absolute evidence of nonlocal correlations, our experimental configuration and timing condition are similar to that used in many EPR experiments. Our

results suggest that an experimental demonstration of the angular EPR paradox [33] should be possible.

#### ACKNOWLEDGMENTS

We thank Monika Ritsch-Marte for helpful discussions. This work was supported by the UK EPSRC, the Royal Society, the Wolfson Foundation, the Leverhulme Trust, the US DoD, MURI, and AFOSR.

- 
- [1] J. F. Clauser, Phys. Rev. Lett. **36**, 1223 (1976).
  - [2] A. Aspect, J. Dalibard, and G. Roger, Phys. Rev. Lett. **49**, 1804 (1982).
  - [3] D. T. Pegg, D. M. Dodderell, and Robin Bendall, J. Chem. Phys. **77**, 2745 (1982).
  - [4] M. Nielsen and I. L. Chuang, *Quantum Computation and Quantum Information* (Cambridge University Press, Cambridge, 2000).
  - [5] J. G. Rarity and P. R. Tapster, Phys. Rev. Lett. **64**, 2495 (1990).
  - [6] L. Mandel and E. Wolf, *Optical Coherence and Quantum Optics* (Cambridge University Press, Cambridge, 1995).
  - [7] D. V. Strekalov, A. V. Sergienko, D. N. Klyshko, and Y. H. Shih, Phys. Rev. Lett. **74**, 3600 (1995).
  - [8] J. C. Howell, R. S. Bennink, S. J. Bentley, and R. W. Boyd, Phys. Rev. Lett. **92**, 210403 (2004).
  - [9] L. Allen, M. W. Beijersbergen, R. J. C. Spreeuw, and J. P. Woerdman, Phys. Rev. A **45**, 8185 (1992).
  - [10] M. J. Padgett, J. Courtial, and L. Allen, Phys. Today **57**, 35 (2004).
  - [11] A. Mair, A. Vaziri, G. Weihs, and A. Zeilinger, Nature (London) **412**, 313 (2001).
  - [12] H. H. Arnaut and G. A. Barbosa, Phys. Rev. Lett. **85**, 286 (2000).
  - [13] S. S. R. Oemrawsingh, X. Ma, D. Voigt, A. Aiello, E. R. Eliel, G. W. 't Hooft, and J. P. Woerdman, Phys. Rev. Lett. **95**, 240501 (2005).
  - [14] S. M. Barnett and D. T. Pegg, Phys. Rev. A **41**, 3427 (1990).
  - [15] E. Yao, S. Franke-Arnold, J. Courtial, S. M. Barnett, and M. J. Padgett, Opt. Express **14**, 9071 (2006).
  - [16] J. B. Pors, A. Aiello, S. S. R. Oemrawsingh, M. P. van Exter, E. R. Eliel, and J. P. Woerdman, Phys. Rev. A **77**, 033845 (2008).
  - [17] R. Zambrini and S. M. Barnett, Phys. Rev. Lett. **96**, 113901 (2006).
  - [18] S. Franke-Arnold, S. M. Barnett, E. Yao, J. Leach, J. Courtial, and M. Padgett, New J. Phys. **6**, 103 (2004).
  - [19] J. Leach, J. Courtial, K. Skeldon, S. M. Barnett, S. Franke-Arnold, and M. J. Padgett, Phys. Rev. Lett. **92**, 013601 (2004).
  - [20] V. V. Bazhenov, M. V. Vasnetsov, and M. S. Soskin, JETP Lett. **52**, 429 (1990).
  - [21] E. Yao, S. Franke-Arnold, J. Courtial, and M. J. Padgett, Opt. Express **14**, 13089 (2006).
  - [22] M. Stutz, S. Gröblacher, T. Jennewein, and A. Zeilinger, Appl. Phys. Lett. **90**, 261114 (2007).
  - [23] R. Ghosh, C. K. Hong, Z. Y. Ou, and L. Mandel, Phys. Rev. A **34**, 3962 (1986).
  - [24] J. Arlt, K. Dholakia, L. Allen, and M. J. Padgett, Phys. Rev. A **59**, 3950 (1999).
  - [25] M. J. Padgett and L. Allen, Opt. Commun. **121**, 36 (1995).
  - [26] J. P. Torres, A. Alexandrescu, and L. Torner, Phys. Rev. A **68**, 050301(R) (2003).
  - [27] S. Franke-Arnold, S. M. Barnett, M. J. Padgett, and L. Allen, Phys. Rev. A **65**, 033823 (2002).
  - [28] G. Molina-Terriza, J. P. Torres, and L. Torner, Opt. Commun. **228**, 155 (2003).
  - [29] D. N. Klyshko, *Photons and Nonlinear Optics* (Gordon and Breach, New York, 1988).
  - [30] E. K. Tan, J. Jeffers, S. M. Barnett, and D. T. Pegg, Eur. Phys. J. D **22**, 495 (2003).
  - [31] J. Leach, M. R. Denis, J. Courtial, and M. J. Padgett, New J. Phys. **7**, 55 (2005).
  - [32] M. T. Gruneisen, W. A. Miller, R. C. Dymale, and A. M. Sweiti, Appl. Opt. **47**, A33 (2008).
  - [33] J. B. Götte, S. Franke-Arnold, and S. M. Barnett, J. Mod. Opt. **53**, 627 (2006).